Title

The G protein–coupled receptor P2RY8 and follicular dendritic cells promote germinal center confinement of B cells, whereas S1PR3 can contribute to their dissemination

Journal

Journal of Experimental Medicine, 212(13)

ISSN

0022-1007

Authors

Muppidi, Jagan R
Lu, Erick
Cyster, Jason G

Publication Date

2015-12-14

DOI

10.1084/jem.20151250

Peer reviewed

The G protein–coupled receptor P2RY8 and follicular dendritic cells promote germinal center confinement of B cells, whereas S1PR3 can contribute to their dissemination

Jagan R. Muppidi,[1,2,3] Erick Lu,[1,3] and Jason G. Cyster[1,3]

[1]Department of Microbiology and Immunology, [2]Department of Medicine, and [3]Howard Hughes Medical Institute, University of California, San Francisco, San Francisco, CA 94143

The orphan Gα13-coupled receptor P2RY8 is mutated in human germinal center (GC)–derived lymphomas and was recently found to promote B cell association with GCs in a mouse model. Here we establish that P2RY8 promotes clustering of activated B cells within follicles in a follicular dendritic cell (FDC)–dependent manner. Although mice lack a P2RY8 orthologue, we show that mouse GC B cell clustering is also dependent on FDCs acting to support the function of a Gα13-coupled receptor. Mutations in *GNA13* and its downstream effector *ARHGEF1* are associated with the development of disseminated GC-derived lymphomas. We find that egress of *Gna13* mutant GC B cells from lymph nodes in the mouse depends on sphingosine-1-phosphate receptor-3. These findings provide evidence that FDCs promote GC confinement of both human and mouse GC B cells via Gα13-dependent pathways, and they show that dissemination of Gα13-deficient GC B cells additionally requires an egress-promoting receptor.

The Journal of Experimental Medicine

Germinal centers (GCs) are organized as discrete, tightly confined clusters of GC B cells and T follicular helper cells (Tfh cells) in the center of reactive (secondary) follicles. Confinement of GC B cells to the GC is important for fostering interactions with antigen-loaded follicular DCs (FDCs) and Tfh cells during the selection events necessary for antibody affinity maturation (Victora and Nussenzweig, 2012). The sphingosine-1-phosphate receptor S1pr2 is a G protein–coupled receptor (GPCR) that is highly up-regulated on GC B cells and signals via the G protein Gα13 and the RhoGEF Arhgef1 (also known as p115 RhoGEF or Lsc) to inhibit cell migration in response to chemoattractants (Green et al., 2011; Muppidi et al., 2014). S1P is abundant in lymph and blood, rapidly degraded in interstitial fluids by the action of membrane phosphatases and an intracellular lyase, and thought to exist in a decaying gradient from the outer to the center follicle (Green et al., 2011; Cyster and Schwab, 2012). S1pr2 promotes GC B cell and Tfh cell confinement to the follicle center, most likely by inhibiting migration into regions of high S1P (Green et al., 2011; Moriyama et al., 2014; Muppidi et al., 2014). Maintenance of the follicular S1P gradient appears to occur in the absence of FDCs (Wang et al., 2011). However, S1pr2 deficiency does not lead to a complete dispersal of GC B cells or to their appearance in circulation, suggesting that additional factors act to promote GC B cell confinement.

Deficiency in Gα13 and Arhgef1 in the mouse is also associated with loss of local GC B cell confinement, and these deficiencies lead to appearance of GC B cells in lymph and blood (Muppidi et al., 2014). The more penetrant effect of Gα13 deficiency than S1pr2 deficiency led us to identify a second human receptor, P2RY8, that can act via Gα13 to promote B cell association with GCs (Muppidi et al., 2014). Although human P2RY8 is active when expressed in the mouse, the *P2RY8* gene is located on a portion of the pseudoautosomal region of the X chromosome that is lost in rodents, and no orthologues have been identified in the mouse. Because Gα13 signaling in B cells inhibits migration, the GC clustering activity of P2RY8 suggests that the P2RY8 ligand might, like S1P, be more abundant in the outer follicle than in the follicle center. Although the identity of the P2RY8 ligand is unknown, in this study, we take advantage of the ability of P2RY8 overexpression to direct cell movements in the mouse to dissect cellular requirements for controlling ligand distribution.

Loss of function mutations of *S1PR2*, *P2RY8*, *GNA13* (encoding Gα13), and *ARHGEF1* are frequently found in human lymphomas derived from GC B cells (GC B cell–like diffuse large B cell lymphoma [GCB-DLBCL] and Burkitt lymphoma [BL]; Morin et al., 2011; Lohr et al., 2012; Schmitz et al., 2012; Muppidi et al., 2014). These malignancies are considered systemic diseases in humans, and spread of the malignant GC B cells to distant sites such as BM is associated with poor prognosis (Sehn et al., 2011). It is currently unclear

Correspondence to Jason G. Cyster: Jason.Cyster@ucsf.edu

Abbreviations used: DTR, DTx receptor; DTx, diphtheria toxin; DZ, dark zone; FDC, follicular DC; GC, germinal center; GPCR, G protein–coupled receptor; LT, lymphotoxin; LZ, light zone; mLN, mesenteric LN; qPCR, quantitative PCR; Tfh cell, T follicular helper cell.

The Rockefeller University Press $30.00
J. Exp. Med. 2015 Vol. 212 No. 13 2213–2222
www.jem.org/cgi/doi/10.1084/jem.20151250

whether Gα13 deficiency itself is sufficient to promote GC B cell egress or whether loss of Gα13 signaling allows other promigratory signals to dominate and promote egress.

In this study, we sought to further define how GC B cells are normally confined to the GC niche and to understand how GC B cells carrying mutations typical of GC lymphomas undergo systemic spread. We demonstrate that FDCs are required for the function of human P2RY8 in promoting cell clustering at the center of mouse lymphoid follicles. Although P2RY8 is not present in the mouse, we find that FDCs act via a Gα13-dependent mechanism to promote clustering of mouse GC B cells and prevent their egress into lymph. Finally, we show that egress of Gα13-deficient mouse GC B cells is promoted by the promigratory S1P receptor S1pr3.

RESULTS AND DISCUSSION

FDCs are required for P2RY8-mediated GC confinement

We took advantage of our finding that human P2RY8 is active when expressed in the mouse to determine the cell types that influence ligand distribution in vivo and allow P2RY8 to function. Retroviral transduction of P2RY8 in activated mouse B cells caused cells to position in and around GCs after transfer into SRBC-immunized hosts in contrast to control-transduced B cells, which were evenly distributed throughout the follicle and excluded from GCs (Fig. 1 A; Muppidi et al., 2014). When P2RY8-transduced B cells were found in the GC, they appeared to be preferentially positioned in the light zone (LZ) near FDCs (Fig. 1 B and not depicted). To test whether a preexisting GC was required for P2RY8-dependent positioning at the center of the follicle, we transferred vector- or P2RY8-transduced activated B cells into CD19-deficient animals that lack splenic GCs (Rickert et al., 1995). Lack of GL7 staining confirmed an absence of GCs in CD19-deficient animals (Fig. 1 B). Primary follicle FDCs, however, appeared normal in distribution, as seen by CD35 staining (Fig. 1 B). In the absence of GCs, P2RY8 overexpression was able to cause B cells to be positioned at the center of the follicle, over the FDC network, whereas vector-transduced B cells were positioned evenly throughout the follicle (Fig. 1 B). Much smaller numbers of P2RY8-transduced cells could also be seen in the marginal zone and T zone. These findings established that the GC itself was not required for P2RY8-mediated guidance to the follicle center. Given that P2RY8-transduced cells appeared to preferentially position near FDCs in both primary follicles and in GCs, we hypothesized that FDCs were required for P2RY8-mediated follicle center confinement.

Lymphotoxin (LT) signaling is required for FDC survival, and one effect of short-term LT blockade is loss of FDCs (Mackay et al., 1997). We transferred vector- or P2RY8-transduced activated B cells into hosts that had been treated for 1 wk with LTβ receptor fused to human IgG Fc (LTβR-Fc) to block LT signaling or with human IgG as a control. Whereas LT blockade had little effect on positioning of vector-transduced B cells, P2RY8-mediated clustering of B cells at the follicle center was nearly completely disrupted and P2RY8-transduced cells were found scattered with the endogenous B cells and in the T zone (Fig. 1 C). As a second test of the FDC requirement, we generated BM chimeras using hosts that expressed cre-recombinase under control of the CD21 promoter (CD21-cre) and the diphtheria toxin (DTx) receptor (DTR) downstream of a floxed stop element in the ROSA26 locus (CD21-DTR mice; Wang et al., 2011). In these BM chimeras, the DTR is expressed in nonhematopoietic CD21-expressing cells. Recent work has shown that, in addition to FDCs, CD21-cre is expressed in a further population of stromal cells termed "versatile stromal cells (VSCs)" that can take on FDC characteristics in inflamed peripheral LNs (Jarjour et al., 2014). In unimmunized mice, VSCs are situated in the T zone, limiting the follicular effect of DTx-mediated cell ablation to loss of FDCs. P2RY8- or vector-transduced B cells were transferred into control or CD21-DTR reverse BM chimeras that were then treated for 1 d with DTx. Acute FDC ablation prevented P2RY8-mediated clustering at the center of the follicle (Fig. 1 D).

Unimmunized Cxcl13-deficient mice lack FDCs as the result of low expression of surface LTα1β2 on naive B cells (Ansel et al., 2000). After immunization, LT expression by GC B cells can drive FDC development in the absence of Cxcl13, although these FDCs are small and misplaced. To determine whether ectopic FDCs could drive P2RY8-dependent cellular clustering, we transferred vector- or P2RY8-transduced B cells into immunized Cxcl13-deficient mice. In the absence of Cxcl13, ectopic FDCs were sufficient to promote P2RY8-dependent B cell clustering (Fig. 1 E).

Collectively, these data show that FDCs are necessary and sufficient for P2RY8-dependent positioning of B cells in the GC niche. Given that P2RY8 is a Gα13-coupled receptor (Muppidi et al., 2014) and Gα13-coupled receptors are migration inhibitory in B cells, we predict that the P2RY8 ligand is high in the outer follicle and low in the center of follicle, possibly because of ligand degradation or lack of ligand production by FDCs. Our positioning experiments also predict that the P2RY8 ligand is low in marginal zone and T zone.

In addition to containing B cells, GC LZs contain Tfh cells. Tfh cells in the GC express high levels of Bcl6 and CXCR5 (GC-Tfh), in contrast to Tfh cells outside the GC that express intermediate levels of both Bcl6 and CXCR5 (pre-GC Tfh; Crotty, 2011). By quantitative PCR (qPCR) analysis, *P2RY8* was strongly up-regulated in CXCR5-high $CD4^+$ T cells from human tonsil but not CXCR5-intermediate or $CXCR5^-$ $CD4^+$ T cells (Fig. 1 F). In contrast to findings for Tfh cells associated with primary GC responses in mouse LNs (Moriyama et al., 2014), human tonsil GC-Tfh did not up-regulate *S1PR2* (Fig. 1 F). Tonsil GCs are thought to be chronically stimulated, and in this regard, it is notable that Tfh cells associated with secondary GCs in the mouse have a different gene expression profile compared with those associated with primary GCs, including somewhat lower S1pr2 expression (Suan et al., 2015). We speculate that

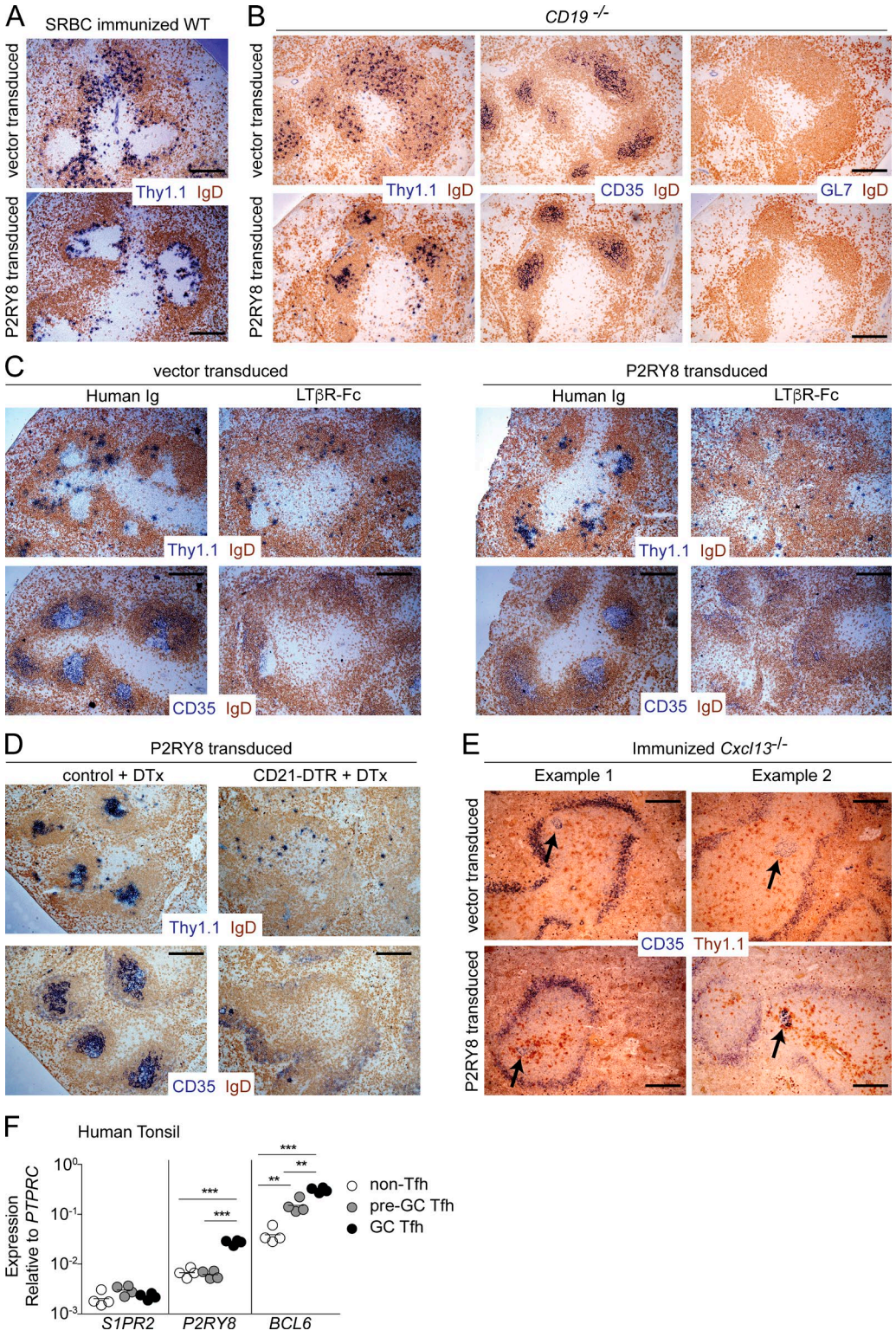

Figure 1. **FDCs are required for P2RY8-dependent confinement to the center of the follicle.** (A–E) Activated *Gpr183*$^{+/-}$ B cells (see Materials and methods) were transduced with retroviral vector encoding Thy1.1 alone (vector) or P2RY8 and Thy1.1 and transferred into WT animals previously immunized with sheep red blood cells (SRBC; A), CD19-deficient animals lacking splenic GCs (B), WT animals treated with LTβR-Fc or human IgG for 1 wk (C), CD21-DTR or littermate control reverse BM chimeras treated with DTx at the time of transfer (D), or previously immunized *Cxcl13*$^{-/-}$ animals (E, arrows indicate ectopic FDC; two images are shown for each condition). Spleens were harvested 1 d after transfer and analyzed immunohistochemically for the presence

P2RY8 may have a prominent and nonredundant role in Tfh cell positioning in LZs of chronically stimulated human GCs.

FDCs prevent dispersal and egress of GC B cells via Gα13

Although a P2RY8 orthologue does not exist in the mouse, our past work established that mouse S1pr2 deficiency does not phenocopy Gα13 deficiency in terms of egress of GC B cells into circulation (Muppidi et al., 2014). This suggested that an additional cue, possibly related to the ones acting via P2RY8, functions in the mouse to promote confinement of GC B cells via Gα13. Consistent with this logic, previous work from our laboratory suggested that S1pr2 cooperated with FDCs to promote confinement of GC B cells within follicles in mesenteric LNs (mLNs; Wang et al., 2011). To address the role of FDCs in promoting mouse GC B cell confinement and in preventing egress of GC B cells into lymph, we tested the effect of FDC ablation using CD21-DTR reverse BM chimeras. DTx treatment of CD21-DTR reverse BM chimeras results in a rapid reduction in GC B cells, likely as a result of the loss of prosurvival factors provided by FDCs to GC B cells (Wang et al., 2011). Therefore, to assess the role of FDCs in GC confinement and to reduce the influence of loss of these prosurvival cues, we generated littermate control and CD21-DTR reverse BM chimeras using *BCL2*-tg BM in which BCL2 is overexpressed in B cells. FDC ablation in these chimeras led to minimal change in mLN GC B cell numbers, and it did not lead to an increase in GC B cells in lymph (Fig. 2 A). Immunohistochemical analysis showed that GC B cells in the DTx-treated mice remained confined to their niche at the follicle center despite the absence of FDCs (Fig. 2 B). To quantify GC B cell dispersal, we developed an algorithm to calculate the area within a follicle where GC B cells were intermixed with naive follicular B cells in immunohistochemical images (see Materials and methods and Fig. S1 A). We defined the GC dispersal index as the area within the follicle where IgD and GL7 staining were intermixed. This measure was very consistent across a number GCs of varying sizes from mLNs of WT animals such that confined GCs typically have a GC dispersal index of 0.18 (Fig. S1, B and C). When we applied this algorithm to control and FDC-ablated *BCL2*-tg BM chimeras, we found that after FDC ablation, there was no loss of GC confinement (Fig. 2 B, right; and Fig. S1 D). These observations are consistent with S1pr2 being able to act as a confinement receptor even in the absence of FDCs.

S1pr2-deficient GC B cells have enhanced survival compared with WT cells (Green et al., 2011) and they are also resilient to loss after FDC ablation (Fig. 2 C, left; Wang et al., 2011). However, in contrast to the findings in *BCL2*-tg chimeras, the S1pr2-deficient GC B cells became dispersed throughout the mLNs after FDC ablation (Fig. 2 D and Fig. S1 E). Importantly, FDC ablation also promoted the egress of S1pr2-deficient GC B cells into lymph (Fig. 2 C, right). To determine whether egress of S1pr2-deficient GC B cells into lymph after FDC ablation was caused by loss of an additional input into Gα13 in GC B cells, we reconstituted lethally irradiated control or CD21-DTR reverse BM chimeras using BM from mice with a B cell–specific deletion of *Gna13*. In the control BM chimeras there was already dispersal of GC B cells through the follicles and appearance of significant numbers of GC B cells in lymph (Fig. 2, E and F; and Fig. S1 F), consistent with our earlier data (Muppidi et al., 2014). Importantly, FDC ablation did not result in greater dispersal of Gα13-deficient GC B cells histologically (Fig. 2 F and Fig. S1 F) or to greater dissemination of Gα13-deficient GC B cells into lymph (Fig. 2 E). These data suggest that FDCs cooperate with S1pr2 to promote follicle center confinement and prevent egress of mouse GC B cells via a Gα13-dependent mechanism.

Egress of Gα13-deficient GC B cells into circulation is mediated by S1pr3

It was unclear whether the loss of Gα13 signaling itself was sufficient to drive GC B cells into circulation or whether the loss of Gα13 allowed other promigratory cues in GC B cells to dominate and thereby promote egress. In considering this issue, we noted that the disruption of GC architecture in the absence of Gα13 sometimes appeared most evident in GCs that were closest to the LN capsule, with extensive spreading of GC B cells throughout the follicle (Fig. 3 A, arrows and inset). This led us to speculate that a factor that was abundant in lymphatic sinuses was promoting a greater degree of spreading of GC B cells in follicles, and possibly egress of GC B cells from the mLN into circulation.

Previous work has established that S1P concentrations are high in lymph and blood and are much lower within lymphoid tissue. We hypothesized that S1P could be present in higher amounts in follicles near lymph-filled subcapsular and cortical sinuses (Cyster and Schwab, 2012). We have previously shown in vitro that S1P inhibits chemokine-induced migration of WT GC B cells via the action of S1pr2 and Gα13, and it cannot induce their migration even when used at high concentrations that efficiently promote migration of other lymphocyte populations (Green et al., 2011; Muppidi et al., 2014). Paradoxically, in the absence of Gα13 or Arhgef1, S1P became promigratory for GC B cells (Fig. 3 B and not depicted). Several S1P receptors have been shown to promote migration toward S1P (Cyster and Schwab, 2012). S1pr1 (also

of transduced cells (Thy1.1), FDCs (CD35), GC B cells (GL7), or naive follicular B cells (IgD) as indicated. Bars, 100 µm. Images are representative of four, two, two, two, and three independent experiments, respectively. (F) qPCR of *S1PR2*, *P2RY8*, and *BCL6* from CXCR5$^-$ (non-Tfh), CXCR5 intermediate (pre-GC Tfh), and CXCR5-high (GC Tfh) CD4$^+$ T cells from human tonsil. Data are from four donors and lines indicate means. **, $P < 0.01$; ***, $P < 0.001$, unpaired two-tailed Student's *t* test.

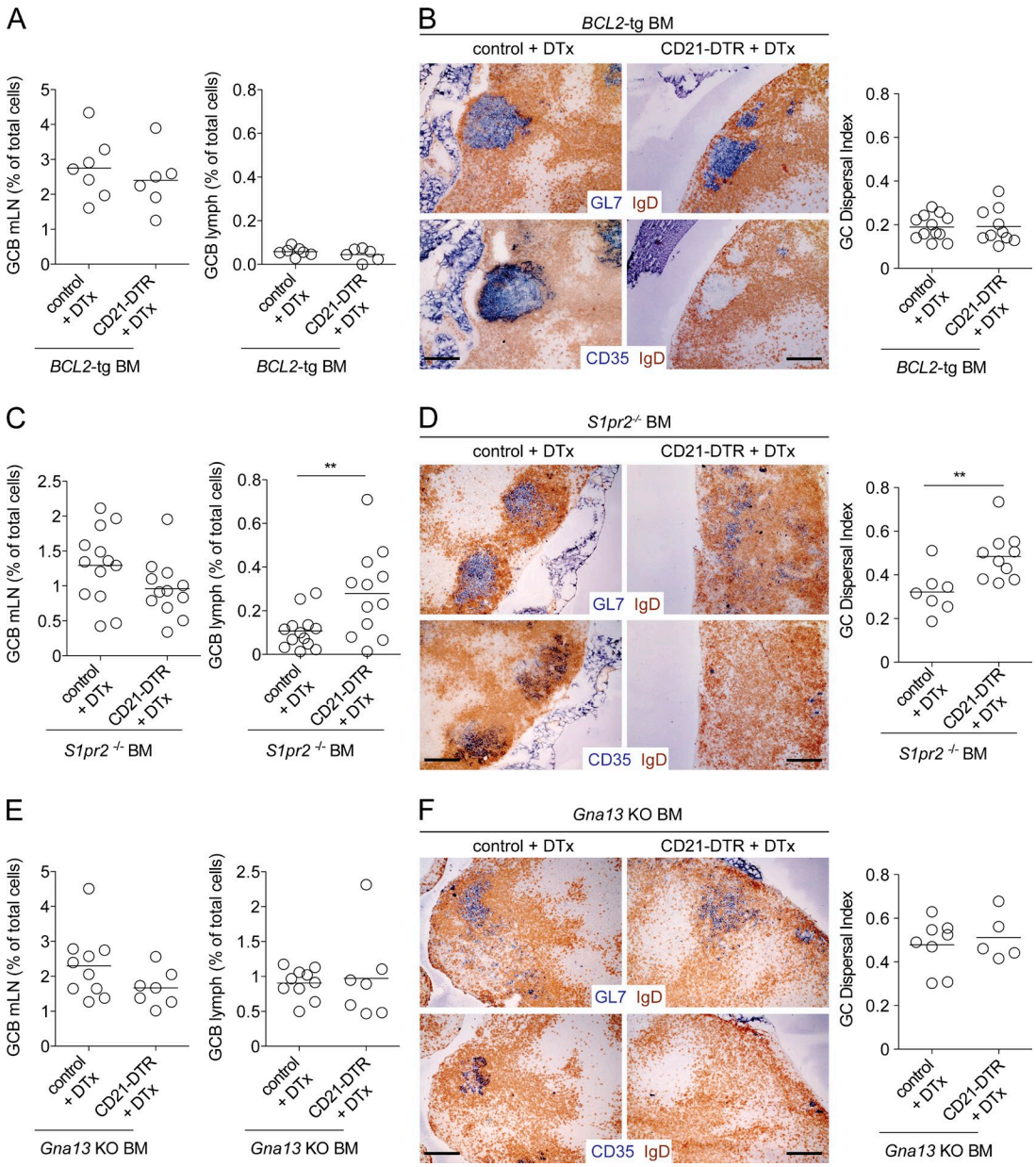

Figure 2. **FDCs cooperate with S1pr2 to promote Gα13–dependent confinement of mLN GC B cells.** (A–F) CD21-DTR or control mice were reconstituted with *BCL2*-tg (A and B), *S1pr2*$^{-/-}$ (C and D), or *Gna13* KO (*f/f mb1-cre*; E and F) BM. Chimeras were treated with 100 ng DTx i.p., and 16–20 h later the frequency of GC B cells in mLNs and lymph was analyzed by FACS (A, C, and E) or mLNs were analyzed immunohistochemically (B, D, and F) for the presence of GC B cells (GL7, top) or FDCs (CD35, bottom). Bars, 100 µm. The GC dispersal index was calculated within individual follicles by analyzing the area of the follicle with intermixing of GL7 and IgD stains (see Materials and methods and Fig. S1). A, C, and E are pooled data from two, four, and two independent experiments, respectively, with two to four mice per group in each experiment. Images in B, D, and F are representative of two, three, and two mice of each type, respectively. In dot plots in A, C, and E, dots indicate individual mice and lines indicate means. In dot plots in B, D, and F, dots indicate the GC dispersal index within an individual follicle and lines indicate means. **, $P < 0.01$, unpaired two-tailed Student's *t* test.

known as $S1P_1$ or Edg1) is the best characterized of these promigratory S1P receptors. However, unlike naive follicular B cells that express high levels of S1pr1 and migrate toward S1P in an S1pr1-dependent fashion, S1pr1 is transcriptionally down-regulated in GC B cells (Green et al., 2011). To exclude the possibility that low-level S1pr1 expression was sufficient to promote egress of GC B cells into circulation, we treated Arhgef1-deficient mixed BM chimeras with the S1pr1 functional antagonist, FTY720, and assessed lymph for the presence of GC B cells. As expected, given the known role of S1pr1 in promoting egress of follicular B cells into circulation (Matloubian et al., 2004), there was a large reduction

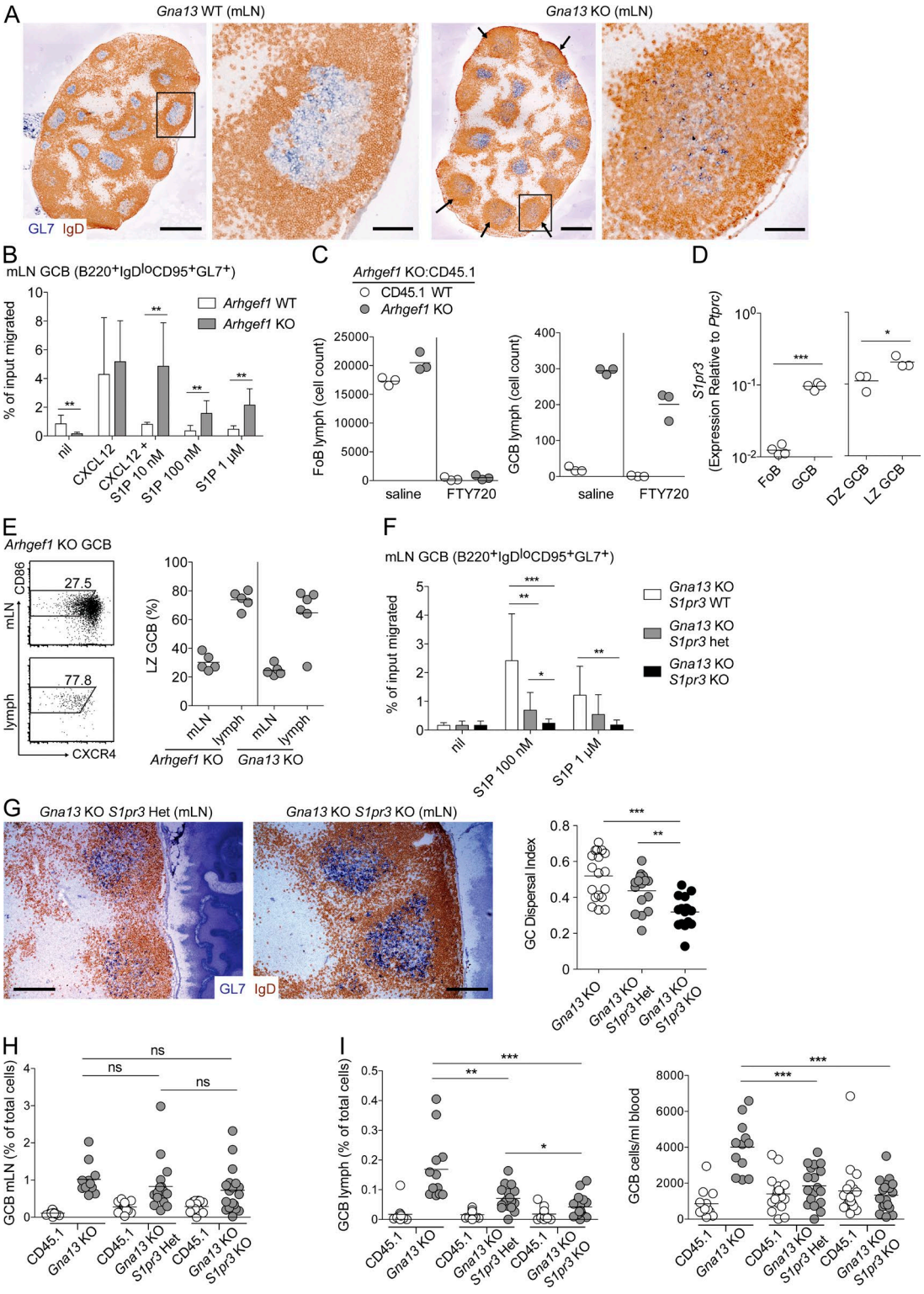

Figure 3. **S1pr3 is required for egress of Gα13-deficient GC B cells into circulation.** (A) Immunohistochemical analysis of mLNs from *Gna13* WT (*f/+*) or KO (*f/f mb1-cre*) animals stained to detect GC B cells (GL7) and naive follicular B cells (IgD). Arrows indicate subcapsular GCs with greatest degree of dispersal. Black boxes indicate GC shown in enlarged image to the right. Data are representative of at least four animals of each type. (B) Transwell migration of *Arhgef1* WT or KO GC B cells to 100 ng/ml CXCL12 in the presence or absence of S1P, or to S1P alone, at the indicated concentrations. Shown are pooled data from four independent experiments. (C) Lymph was collected from *Arhgef1* mixed chimeras treated with 1 mg/kg FTY720 or saline i.p. for 3 h

in the number of both Arhgef1-deficient and CD45.1 WT follicular B cells in lymph after FTY720 treatment (Fig. 3 C, left). However, the number of Arhgef1-deficient GC B cells in lymph after FTY720 was only slightly decreased (Fig. 3 C, right), suggesting that S1pr1 is not principally responsible for egress of Gα13- or Arhgef1-deficient GC B cells.

S1pr3, a second S1P receptor that can couple to Gαi and have promigratory effects (Cinamon et al., 2004), is up-regulated on mouse GC B cells relative to follicular B cells (Fig. 3 D). In agreement with studies comparing genome-wide LZ and dark zone (DZ) GC B cell gene expression (Victora et al., 2010; unpublished data), S1pr3 is up-regulated on LZ relative to DZ GC B cells (Fig. 3 D). Consistent with the possibility that S1pr3 promotes egress of mouse Gα13- or Arhgef1-deficient GC B cells into circulation, we found that the majority of Gα13- or Arhgef1-deficient GC B cells in lymph from mixed chimeras were LZ phenotype (Fig. 3 E). To determine whether S1pr3 supported migration of Gα13-deficient GC B cells toward S1P, we generated B cell–specific Gα13-deficient mice that were also deficient for S1pr3. In the absence of S1pr3, Gα13-deficient GC B cells could not migrate toward S1P, and cells lacking one copy of S1pr3 showed an intermediate defect in their migratory response (Fig. 3 F). Histologically, Gα13-deficient GC B cells demonstrated a partial rescue in their confinement when they also lacked S1pr3 (Fig. 3 G). Histological quantification of multiple follicles showed a wide range of GC dispersal in the absence of Gα13 that was reduced by the additional absence of S1pr3 (Fig. 3 G, right; and Fig. S1 G). In mixed BM chimeras Gα13/S1pr3 double-deficient GC B cells outgrew their WT counterparts to a similar extent as Gα13 single-deficient GC B cells (Fig. 3 H). However, when we examined circulatory fluids of these mixed chimeras, we found that loss of S1pr3 was sufficient to prevent egress of Gα13-deficient GC B cells into lymph and blood (Fig. 3 I). Although in the absence of one copy of *S1pr3* there was only a small nonstatistically significant reduction in GC dispersal histologically, *S1pr3* heterozygosity led to a significant reduction in GC B cell appearance in lymph (Fig. 3, G [right] and I). Previous studies have established that under conditions when cells are responding to multiple opposing promigratory inputs, heterozygosity in chemoattractant receptor expression can have a strong impact on the response (Cinamon et al., 2004; Ekland et al., 2004; Pham et al., 2008; Meechan et al., 2012; McDermott et al., 2015). These data provide evidence that in the absence of Gα13 signaling, S1P acts via S1pr3 to promote the egress of mouse GC B cells into circulation.

Concluding remarks

In summary, we find that FDCs promote confinement of B cells to the GC niche via a Gα13-dependent mechanism. Our studies suggest that in humans this involves P2RY8, whereas in mouse the nature of the Gα13-coupled receptor involved is not yet defined. We speculate that although mice lack a P2RY8 orthologue, the same conserved ligand acts on the unidentified mouse receptor to promote Gα13 signaling in GC B cells. We suggest a model in which a broadly distributed small molecule GPCR ligand is degraded or inactivated by FDCs, causing these cells to act as a "sink" and make the follicle center a low point in the ligand field, allowing the migration-inhibitory Gα13-coupled receptor to promote confinement of cells to this region. The EBI2 ligand 7α,25-dihydroxycholesterol (7α,25-HC) provides precedent for a GPCR ligand being abundant at the outer follicle and being maintained in low abundance in the follicle center in an FDC-dependent manner (Yi et al., 2012). P2RY8 does not show migration inhibition by 7α,25-HC, and the ability of this receptor to promote follicle center clustering of B cells was not interrupted in Cyp7b1-deficient mice that lack 7α,25-HC (unpublished data). We suggest that another small molecule is similarly distributed through related mechanisms. Although our and most published studies show that Gα13-coupled receptors mediate migration inhibition, rare examples of Gα13 having a promigratory role have been reported in fibroblasts and epithelial cells (Shan et al., 2006; Yagi et al., 2011), and we cannot exclude the possibility that P2RY8 has a promigratory role and that FDCs are a source of P2RY8 attractant.

We also show that LN egress of Gα13-deficient mouse GC B cells occurs via the up-regulation of S1pr3 on LZ cells. We suggest a model in which S1P-S1pr2 signaling in GC B cells via Gα13 and Arhgef1 normally dominates the S1P response of GC B cells and helps mediate their GC confinement. However, when this migration-inhibitory signaling pathway is lacking, S1pr3 can dominate the S1P response and allow cells that have entered the follicle to be guided

and analyzed for the presence of follicular (FoB) or GC B cells. Data are from one experiment representative of two. (D) qPCR of *S1pr3* in sorted FoB, total GC B, LZ GC B, and DZ GC B. Shown are pooled data from three independent experiments. (E) mLNs or lymph from *Arhgef1* or *Gna13* KO mixed chimeras were analyzed by FACS for the presence of LZ phenotype GC B cells. Left panels show example FACS plots, and the right panel summarizes data from three experiments. (F) Transwell migration of *Gna13* KO GC B cells that were WT, heterozygous, or deficient for S1pr3. Assay was performed as in B. Shown are pooled data from five independent experiments. (G) Immunohistochemical analysis of mLNs from *Gna13* KO *S1pr3* WT, heterozygous, or KO animals, stained as in A. Data are representative of three mice of each type. GC dispersal index of individual follicles was calculated as described in Materials and methods and Fig. S1. Bars: (A, whole LNs) 500 µm; (A [enlarged GCs] and G) 100 µm. (H and I) Percentages of GC B cells from mLN (H) lymph or blood (I) from mixed BM chimeras that were reconstituted with ∼60% WT CD45.1 and ∼40% *Gna13* KO BM that was also WT, heterozygous, or deficient for *S1pr3*. Data are pooled from three independent experiments. In dot plots in C–E, H, and I, dots indicate individual mice and lines indicate means. In the dot plot in G, dots indicate the GC dispersal index in individual follicles and lines indicate means. In B and F, error bars show SD. *, $P < 0.05$; **, $P < 0.01$; ***, $P < 0.001$, unpaired two-tailed Student's *t* test.

into subcapsular or cortical sinuses for LN egress. Although S1PR3 is not up-regulated in human tonsillar GC B cells (Victora et al., 2012; unpublished data), we speculate that a similar egress-promoting receptor is required for egress of *GNA13* or *ARHGEF1* mutant human GC B cells. Identification of this human receptor may provide opportunities to inhibit the dissemination of GCB-DLBCL or BL cells.

Efficient selection of high-affinity clones in the GC requires transitioning of cells between the LZ and DZ. CXCR5 and CXCR4 are the dominant chemotactic inputs mediating transition between these two zones (Allen et al., 2004; Bannard et al., 2013). In initial experiments, we have not observed defects in LZ positioning of S1pr3-deficient GC B cells (unpublished data), consistent with S1pr2 dominating the S1P response of these cells. However, the G protein–coupling properties of S1pr3 are complex (Sanchez and Hla, 2004), and conditions may exist where S1pr3 can dominate over S1pr2 even in WT cells. It will be important to investigate whether S1pr3 is required for optimal function of the GC in supporting selection of high-affinity clones.

In addition to the P2RY8 mutations we and others have previously reported in GC-derived malignancy (Lohr et al., 2012; Schmitz et al., 2012; Muppidi et al., 2014), whole exome sequencing experiments have reported deleterious P2RY8 mutations in gastric, colon, and lung adenocarcinomas (Bamford et al., 2004). Therefore, our findings regarding cellular requirements for determining P2RY8 ligand distribution may be of broader relevance to understanding how P2RY8 loss-of-function contributes to cancer progression.

MATERIALS AND METHODS

Mice and BM chimeras. Adult C57BL6 CD45.1$^+$ (stock number 564) mice at least 7 wk of age were from the National Cancer Institute (NCI) or NCI at CRV. *Gpr183*$^{+/-}$, *Cd19*$^{-/-}$, *Cxcl13*$^{-/-}$, and *Arhgef1*$^{-/-}$ mice were on a B6 background. *CD21-cre* (*Cr2-cre*) and ROSA-DTR mice were on a B6 background and were from The Jackson Laboratory. *S1pr3*$^{-/-}$ mice were on a B6 background, and *S1pr2*$^{-/-}$ mice (Kono et al., 2004) were backcrossed for at least six generations to B6 and were provided by R. Proia (National Institue of Diabetes and Digestive and Kidney Diseases, Bethesda, MD). *Gna13*$^{f/f}$ mice were on a mixed C57BL6/129 background (Ruppel et al., 2005) and were provided by S. Coughlin (University of California, San Francisco). *Mb1-cre* mice (provided by M. Reth, Max Planck Institute of Immunobiology and Epigenetics, Freiburg, Germany) express Cre in all B lineage cells (Hobeika et al., 2006). *BCL2*-tg mice overexpress BCL2 selectively in B cells (Strasser et al., 1991). Mixed BM chimeras were made using Ly5.2 (CD45.1$^+$) from NCI as hosts as described previously (Green et al., 2011) and analyzed at least 6 wk after reconstitution. Mice were housed in a specific pathogen–free environment in the Laboratory Animal Research Center at the University of California, San Francisco, and all animal procedures were approved by the Institutional Animal Care and Use Committee.

Treatments. For LT-blocking experiments, animals were treated with LTβR-Fc (provided by J. Browning, Biogen Idec) using 100 µg on days −7 and −4 before transfer of transduced B cells. FDC ablation was performed as described previously (Wang et al., 2011). In brief, animals expressing CD21-cre and ROSA-DTR alleles or littermate controls were lethally irradiated and reconstituted with WT, *BCL2*-Tg, *S1pr2*$^{-/-}$, or *mb1*-cre *Gna13*$^{f/f}$ BM. 6–8 wk after irradiation, animals were treated with 100 ng DTx (EMD Biosciences) i.p. and analyzed 16–20 h later. *Cxcl13*$^{-/-}$ mice were immunized with 50 µg duck egg lysozyme–ovalbumin in the Sigma-Aldrich Adjuvant system 1 d after transfer of 10^5 Hy10 B cells and 5×10^4 OT-II T cells (Green et al., 2011). Animals were analyzed at day 6 after immunization. For FTY720 experiments, mice were injected i.p. at 1 mg FTY720 (Selleck Chemicals) per kg body weight or an equivalent volume of saline for 3 h.

Retroviral constructs and transductions. The P2RY8 retroviral construct was made as described previously (Muppidi et al., 2014). *Gpr183*$^{+/-}$ spleen cells were harvested in media containing 0.25 µg/ml anti-CD180 (RP-105; clone RP14; BD) and cultured for 24 h. B cells heterozygous for EBI2 (*Gpr183*) were used because the activation conditions used to retrovirally transduce the cells cause up-regulation of this receptor (contrary to its low expression in GC B cells), and we have found previously that EBI2 heterozygosity helps reveal the GC-clustering activity of S1pr2 (Green et al., 2011; Wang et al., 2011; Muppidi et al., 2014). The activated B cells were spin-infected twice on consecutive days for 1.5 h with retroviral supernatant and cultured overnight after the second spin infection before transfer into recipient mice. Transferred cells were analyzed after 24 h by flow cytometry and immunohistochemistry.

Cell isolation, clonality assessment, adoptive transfer, cell culture, treatments, flow cytometry, and qPCR. Cells from spleen, mLNs, and blood were isolated and stained as described previously (Green et al., 2011). Lymph was collected from the cisterna chyli via a fine glass micropipette (Matloubian et al., 2004). Chemotaxis assays of GC B cells were performed using total mLN cells that were RBC lysed twice (Green et al., 2011). Flow cytometry was performed on an LSRII (BD). For GC B cell analysis, cells were stained with APC-Cy7–conjugated anti-B220 (RA3-6B2; BioLegend), BV605-conjugated anti-CD4 (RM4-5; BioLegend), Pacific blue–conjugated anti-IgD (11-26c.2a; BioLegend), PE-Cy7–conjugated anti-CD38 (90; BioLegend), PE-conjugated anti-Fas (Jo2; BD), AF647-conjugated anti-GL7 (GL7; BioLegend), FITC-conjugated anti-CD45.2 (104; BioLegend), PerCP-Cy5.5–conjugated anti-CD45.1 (A20; BioLegend), PerCP-Cy5.5–conjugated anti-CD86 (GL-1; BioLegend), biotinylated anti-CXCR4 (2B11; BD), and/or BV605 conjugated to streptavidin (BioLegend). qPCR was performed as described previously (Bannard et al., 2013) on FACS-sorted GC B cells. For human samples the following primers were used: *P2RY8*, (F) 5′-TGTTTATTACTTT

GCGTCCC-3′ and (R) 5′-ATCCCTTCAGGGTGCGC-3′; *BCL6*, (F) 5′-CGTGAGCAGTTTAGAGCCCA-3′ and (R) 5′-GCAGAATCCCTCAGGGTTGA-3′; *S1PR2*, (F) 5′-GGACGCAGACGCCAAGG-3′ and (R) 5′-CGAGTACA AGCTGCCCATG-3′; and *PTPRC*, (F) 5′-AAACGGAG ATGCAGGGTCAA-3′ and (R) 5′-GTTTCATCCCTGG GACCTTGT-3′. For mouse samples the following primers were used: *S1pr3*, (F) 5′-GGAGCCCCTAGACGGGAGT-3′ and (R) 5′-CCGACTGCGGGAAGAGTGT-3′; and *Ptprc*, (F) 5′-TTCCAAGAGGAAGGAGCCCA-3′ and (R) 5′-AGAACAACCCTGTCTGCTGG-3′.

Immunohistochemical analysis. Cryosections 7 µm in thickness from mLNs and spleen were cut and prepared as described previously (Green et al., 2011). Primary antibodies used for staining cryosections were biotinylated anti-Thy1.1 (CD90.1; HIS51; eBioscience), biotinylated anti-GL7 (GL7; eBioscience), biotinylated or unlabeled anti-CD35 (8C12; BD), and unlabeled polyclonal goat anti–mouse IgD (Cedarlane). Secondary antibodies or streptavidin fused to alkaline phosphatase or peroxidase were from Jackson ImmunoResearch Laboratories, Inc. Images were captured with an AxioObserver Z1 inverted microscope (Carl Zeiss).

Image analysis. Single follicles were cropped from larger images using ImageJ (National Institutes of Health). The IHC Image Analysis Toolbox in ImageJ was used to create separate binary IgD and GL7 images of each follicle. Using MATLAB, each pair of binary images was divided into 25-pixel by 25-pixel boxes, and individual boxes were counted for pixels positive for IgD or GL7. Boxes containing no GL7 or IgD pixels were excluded. For remaining boxes, the proportion of pixels positive for GL7 was calculated by dividing the number of GL7-positive pixels by the sum of IgD- and GL7-positive pixels. The GC dispersal index, calculated in R, was defined as the fraction of boxes within each follicle containing between 1 and 99% of pixels staining positive for GL7 (see Fig. S1 A for example of workflow). MATLAB and R scripts are available upon request.

Statistical analysis. Prism software (GraphPad Software) was used for all statistical analysis. Data were analyzed with a two-sample unpaired (or paired, where indicated) Student's *t* test. P-values were considered significant when ≤ 0.05.

Online supplemental material. Fig. S1 shows the workflow of quantification of GC dispersal from IHC images and pooled analysis of GC dispersal from all conditions analyzed. Online supplemental material is available at http://www.jem.org/cgi/content/full/jem.20151250/DC1.

ACKNOWLEDGMENTS

We thank J. An for maintaining the mouse colony, Y. Xu, Y. Liang, and E. Dang for assistance with qPCR, A. Reboldi for valuable discussions, and L. Rodda and M. Mintz for critical reading of the manuscript.

J.R. Muppidi is supported by a Special Fellow Award from the Leukemia & Lymphoma Society and the National Institutes of Health (NIH; K08CA197367). E. Lu is supported by the National Science Foundation (grant no. 1144247). J.G. Cyster is an Investigator of the Howard Hughes Medical Institute. This work was supported in part by NIH grant AI45073.

The authors declare no competing financial interests.

Submitted: 31 July 2015
Accepted: 30 October 2015

REFERENCES

Allen, C.D.C., K.M. Ansel, C. Low, R. Lesley, H. Tamamura, N. Fujii, and J.G. Cyster. 2004. Germinal center dark and light zone organization is mediated by CXCR4 and CXCR5. *Nat. Immunol.* 5:943–952. http://dx.doi.org/10.1038/ni1100

Ansel, K.M., V.N. Ngo, P.L. Hyman, S.A. Luther, R. Förster, J.D. Sedgwick, J.L. Browning, M. Lipp, and J.G. Cyster. 2000. A chemokine-driven positive feedback loop organizes lymphoid follicles. *Nature.* 406:309–314. http://dx.doi.org/10.1038/35018581

Bamford, S., E. Dawson, S. Forbes, J. Clements, R. Pettett, A. Dogan, A. Flanagan, J. Teague, P.A. Futreal, M.R. Stratton, and R. Wooster. 2004. The COSMIC (Catalogue of Somatic Mutations in Cancer) database and website. *Br. J. Cancer.* 91:355–358.

Bannard, O., R.M. Horton, C.D.C. Allen, J. An, T. Nagasawa, and J.G. Cyster. 2013. Germinal center centroblasts transition to a centrocyte phenotype according to a timed program and depend on the dark zone for effective selection. *Immunity.* 39:912–924. (published erratum appears in *Immunity*. 2013. 39:1182) http://dx.doi.org/10.1016/j.immuni.2013.08.038

Cinamon, G., M. Matloubian, M.J. Lesneski, Y. Xu, C. Low, T. Lu, R.L. Proia, and J.G. Cyster. 2004. Sphingosine 1-phosphate receptor 1 promotes B cell localization in the splenic marginal zone. *Nat. Immunol.* 5:713–720. http://dx.doi.org/10.1038/ni1083

Crotty, S. 2011. Follicular helper CD4 T cells (TFH). *Annu. Rev. Immunol.* 29:621–663. http://dx.doi.org/10.1146/annurev-immunol-031210-101400

Cyster, J.G., and S.R. Schwab. 2012. Sphingosine-1-phosphate and lymphocyte egress from lymphoid organs. *Annu. Rev. Immunol.* 30:69–94. http://dx.doi.org/10.1146/annurev-immunol-020711-075011

Ekland, E.H., R. Forster, M. Lipp, and J.G. Cyster. 2004. Requirements for follicular exclusion and competitive elimination of autoantigen-binding B cells. *J. Immunol.* 172:4700–4708. http://dx.doi.org/10.4049/jimmunol.172.8.4700

Green, J.A., K. Suzuki, B. Cho, L.D. Willison, D. Palmer, C.D.C. Allen, T.H. Schmidt, Y. Xu, R.L. Proia, S.R. Coughlin, and J.G. Cyster. 2011. The sphingosine 1-phosphate receptor $S1P_2$ maintains the homeostasis of germinal center B cells and promotes niche confinement. *Nat. Immunol.* 12:672–680. http://dx.doi.org/10.1038/ni.2047

Hobeika, E., S. Thiemann, B. Storch, H. Jumaa, P.J. Nielsen, R. Pelanda, and M. Reth. 2006. Testing gene function early in the B cell lineage in mb1-cre mice. *Proc. Natl. Acad. Sci. USA.* 103:13789–13794. http://dx.doi.org/10.1073/pnas.0605944103

Jarjour, M., A. Jorquera, I. Mondor, S. Wienert, P. Narang, M.C. Coles, F. Klauschen, and M. Bajénoff. 2014. Fate mapping reveals origin and dynamics of lymph node follicular dendritic cells. *J. Exp. Med.* 211:1109–1122. http://dx.doi.org/10.1084/jem.20132409

Kono, M., Y. Mi, Y. Liu, T. Sasaki, M.L. Allende, Y.-P. Wu, T. Yamashita, and R.L. Proia. 2004. The sphingosine-1-phosphate receptors S1P1, S1P2, and S1P3 function coordinately during embryonic angiogenesis. *J. Biol. Chem.* 279:29367–29373. http://dx.doi.org/10.1074/jbc.M403937200

Lohr, J.G., P. Stojanov, M.S. Lawrence, D. Auclair, B. Chapuy, C. Sougnez, P. Cruz-Gordillo, B. Knoechel, Y.W. Asmann, S.L. Slager, et al. 2012. Discovery and prioritization of somatic mutations in diffuse large B-cell

lymphoma (DLBCL) by whole-exome sequencing. *Proc. Natl. Acad. Sci. USA.* 109:3879–3884. http://dx.doi.org/10.1073/pnas.1121343109

Mackay, F., G.R. Majeau, P. Lawton, P.S. Hochman, and J.L. Browning. 1997. Lymphotoxin but not tumor necrosis factor functions to maintain splenic architecture and humoral responsiveness in adult mice. *Eur. J. Immunol.* 27:2033–2042. http://dx.doi.org/10.1002/eji.1830270830

Matloubian, M., C.G. Lo, G. Cinamon, M.J. Lesneski, Y. Xu, V. Brinkmann, M.L. Allende, R.L. Proia, and J.G. Cyster. 2004. Lymphocyte egress from thymus and peripheral lymphoid organs is dependent on S1P receptor 1. *Nature.* 427:355–360. http://dx.doi.org/10.1038/nature02284

McDermott, D.H., J.L. Gao, Q. Liu, M. Siwicki, C. Martens, P. Jacobs, D. Velez, E. Yim, C.R. Bryke, N. Hsu, et al.. 2015. Chromothriptic cure of WHIM syndrome. *Cell.* 160:686–699. http://dx.doi.org/10.1016/j.cell.2015.01.014

Meechan, D.W., E.S. Tucker, T.M. Maynard, and A.S. LaMantia. 2012. Cxcr4 regulation of interneuron migration is disrupted in 22q11.2 deletion syndrome. *Proc. Natl. Acad. Sci. USA.* 109:18601–18606. http://dx.doi.org/10.1073/pnas.1211507109

Morin, R.D., M. Mendez-Lago, A.J. Mungall, R. Goya, K.L. Mungall, R.D. Corbett, N.A. Johnson, T.M. Severson, R. Chiu, M. Field, et al. 2011. Frequent mutation of histone-modifying genes in non-Hodgkin lymphoma. *Nature.* 476:298–303. http://dx.doi.org/10.1038/nature10351

Moriyama, S., N. Takahashi, J.A. Green, S. Hori, M. Kubo, J.G. Cyster, and T. Okada. 2014. Sphingosine-1-phosphate receptor 2 is critical for follicular helper T cell retention in germinal centers. *J. Exp. Med.* 211:1297–1305. http://dx.doi.org/10.1084/jem.20131666

Muppidi, J.R., R. Schmitz, J.A. Green, W. Xiao, A.B. Larsen, S.E. Braun, J. An, Y. Xu, A. Rosenwald, G. Ott, et al. 2014. Loss of signalling via Gα13 in germinal centre B-cell-derived lymphoma. *Nature.* 516:254–258. http://dx.doi.org/10.1038/nature13765

Pham, T.H., T. Okada, M. Matloubian, C.G. Lo, and J.G. Cyster. 2008. $S1P_1$ receptor signaling overrides retention mediated by $G\alpha_i$-coupled receptors to promote T cell egress. *Immunity.* 28:122–133. http://dx.doi.org/10.1016/j.immuni.2007.11.017

Rickert, R.C., K. Rajewsky, and J. Roes. 1995. Impairment of T-cell-dependent B-cell responses and B-1 cell development in CD19-deficient mice. *Nature.* 376:352–355. http://dx.doi.org/10.1038/376352a0

Ruppel, K.M., D. Willison, H. Kataoka, A. Wang, Y.-W. Zheng, I. Cornelissen, L. Yin, S.M. Xu, and S.R. Coughlin. 2005. Essential role for $G\alpha_{13}$ in endothelial cells during embryonic development. *Proc. Natl. Acad. Sci. USA.* 102:8281–8286. http://dx.doi.org/10.1073/pnas.0503326102

Sanchez, T., and T. Hla. 2004. Structural and functional characteristics of S1P receptors. *J. Cell. Biochem.* 92:913–922. http://dx.doi.org/10.1002/jcb.20127

Schmitz, R., R.M. Young, M. Ceribelli, S. Jhavar, W. Xiao, M. Zhang, G. Wright, A.L. Shaffer, D.J. Hodson, E. Buras, et al. 2012. Burkitt lymphoma pathogenesis and therapeutic targets from structural and functional genomics. *Nature.* 490:116–120. http://dx.doi.org/10.1038/nature11378

Sehn, L.H., D.W. Scott, M. Chhanabhai, B. Berry, A. Ruskova, L. Berkahn, J.M. Connors, and R.D. Gascoyne. 2011. Impact of concordant and discordant bone marrow involvement on outcome in diffuse large B-cell lymphoma treated with R-CHOP. *J. Clin. Oncol.* 29:1452–1457. http://dx.doi.org/10.1200/JCO.2010.33.3419

Shan, D., L. Chen, D. Wang, Y.-C. Tan, J.L. Gu, and X.-Y. Huang. 2006. The G protein $G\alpha_{13}$ is required for growth factor-induced cell migration. *Dev. Cell.* 10:707–718. http://dx.doi.org/10.1016/j.devcel.2006.03.014

Strasser, A., S. Whittingham, D.L. Vaux, M.L. Bath, J.M. Adams, S. Cory, and A.W. Harris. 1991. Enforced BCL2 expression in B-lymphoid cells prolongs antibody responses and elicits autoimmune disease. *Proc. Natl. Acad. Sci. USA.* 88:8661–8665. http://dx.doi.org/10.1073/pnas.88.19.8661

Suan, D., A. Nguyen, I. Moran, K. Bourne, J.R. Hermes, M. Arshi, H.R. Hampton, M. Tomura, Y. Miwa, A.D. Kelleher, et al. 2015. T follicular helper cells have distinct modes of migration and molecular signatures in naive and memory immune responses. *Immunity.* 42:704–718. http://dx.doi.org/10.1016/j.immuni.2015.03.002

Victora, G.D., and M.C. Nussenzweig. 2012. Germinal centers. *Annu. Rev. Immunol.* 30:429–457. http://dx.doi.org/10.1146/annurev-immunol-020711-075032

Victora, G.D., T.A. Schwickert, D.R. Fooksman, A.O. Kamphorst, M. Meyer-Hermann, M.L. Dustin, and M.C. Nussenzweig. 2010. Germinal center dynamics revealed by multiphoton microscopy with a photoactivatable fluorescent reporter. *Cell.* 143:592–605. http://dx.doi.org/10.1016/j.cell.2010.10.032

Victora, G.D., D. Dominguez-Sola, A.B. Holmes, S. Deroubaix, R. Dalla-Favera, and M.C. Nussenzweig. 2012. Identification of human germinal center light and dark zone cells and their relationship to human B-cell lymphomas. *Blood.* 120:2240–2248. http://dx.doi.org/10.1182/blood-2012-03-415380

Wang, X., B. Cho, K. Suzuki, Y. Xu, J.A. Green, J. An, and J.G. Cyster. 2011. Follicular dendritic cells help establish follicle identity and promote B cell retention in germinal centers. *J. Exp. Med.* 208:2497–2510. http://dx.doi.org/10.1084/jem.20111449

Yagi, H., W. Tan, P. Dillenburg-Pilla, S. Armando, P. Amornphimoltham, M. Simaan, R. Weigert, A.A. Molinolo, M. Bouvier, and J.S. Gutkind. 2011. A synthetic biology approach reveals a CXCR4-G13-Rho signaling axis driving transendothelial migration of metastatic breast cancer cells. *Sci. Signal.* 4:ra60. http://dx.doi.org/10.1126/scisignal.2002221

Yi, T., X. Wang, L.M. Kelly, J. An, Y. Xu, A.W. Sailer, J.A. Gustafsson, D.W. Russell, and J.G. Cyster. 2012. Oxysterol gradient generation by lymphoid stromal cells guides activated B cell movement during humoral responses. *Immunity.* 37:535–548. http://dx.doi.org/10.1016/j.immuni.2012.06.015